Self-Sufficient Heterogeneous Biocatalysis through Boronic Acid-Diol Complexation of Adenylated Cofactors

Eleftheria Diamanti[‡1], Susana Velasco-Lozano[‡1,2,3], Daniel Grajales-Hernández[1], Alejandro H. Orrego[1], Desiré Di Silvio[1], José María Fraile[2] and Fernando López-Gallego*[1,4]

[1]Center for cooperative Research in Biomaterials (CIC biomaGUNE) - Basque Research and Technology Alliance (BRTA) Paseo Miramón, 194, 20014 Donostia-San Sebastián, Spain.
[2]Instituto de Síntesis Química y Catálisis Homogénea (ISQCH), CSIC-Universidad de Zaragoza, C/ Pedro Cerbuna, 12, 50009, Zaragoza, Spain.
[3]Aragonese Foundation for Research and Development (ARAID), Av. Ranillas, 1-D, 50018, Zaragoza (Spain)
[4]IKERBASQUE, Basque Foundation for Science, Maria Diaz de Haro 3, 48013 Bilbao, Spain.

KEYWORDS: enzyme immobilization, cis-diol interactions, dehydrogenases, ribose groups, NADH

ABSTRACT

Self-sufficient heterogeneous biocatalysts (ssHB) are promising candidates for implementing cofactor-dependent enzymes in chemical biomanufacturing. Most strategies for co-immobilizing cofactors with dehydrogenases on porous agarose microbeads involve using cationic polymers (i.e., polyethyleneimine-PEI) that interact electrostatically with the phosphate groups of their corresponding phosphorylated cofactors. Although the latter is a powerful and versatile approach, ionic bonds are disrupted in biotransformations operating at high ionic strength, where screening of bonded ions takes place. Harnessing the ribose groups present in adenylated cofactors, we immobilize a selection of these (NAD(P)H, NAD(P)$^+$, FAD, and ATP) on agarose microbeads functionalized with boronic acid to establish reversible covalent bonds between the cis-diol of the ribose in the cofactor backbone and the boronic acid. To do so, we functionalize cobalt-activated porous agarose beads with boronic acid (AG-B/Co^{2+}) for the co-immobilization of adenylated cofactors with the corresponding cofactor dependent His-tagged dehydrogenases. First, we demonstrate that the adenylated cofactor-support interactions are reversible but show resistance against high salt concentrations, overcoming the main limitation of the current self-sufficient heterogeneous biocatalysts. Then, we co-immobilize several His-tagged enzymes with their corresponding adenylated cofactors and investigated the functionality and stability of these ssHBs in reductive aminations performed under high ionic strength both in batch and flow reactors. As a result, we manage to reuse the immobilized enzymes and the cofactors 3.5 x 10^5 and 167 times, respectively. This works expands the usefulness of ssBHs for hitherto bioprocess regardless of the ionic strength of the media.

INTRODUCTION

Industrial biocatalysis is driven by the discovery and engineering of highly efficient enzymes that catalyze both natural and new-to-nature reactions.[1] Most of these enzymes (i.e., dehydrogenases, transaminases, and kinases) depend on exogenous cofactors that form catalytically active holoenzymes, thus many of these cofactors must be exogenously supplied to the reaction media. However, these cofactors are expensive and unstable, hampering the implementation of cofactor-dependent enzymes in industry. In the last decade, our group and others have developed different methodologies to reuse both cofactors and enzymes upon their operational use.[2-5] To this end, one of the most successful approaches is the fabrication

of self-sufficient heterogeneous biocatalysts (ssHBs) where both enzymes and cofactors are immobilized on the same support (solid carrier).[6-8] Hence, biotransformations occur without adding any exogenous cofactor, while the cofactor and the enzyme can be reused by simple filtration or centrifugation once the reaction is completed.

A handful of sophisticated approaches have emerged for cofactor co-immobilization where the cofactor is irreversibly bound through swing arms.[9, 10] However the complexity of these strategies limits the universality of the methodology. For this reason, the co-immobilization of cofactor-dependent enzymes and their cofactors more commonly exploits the reversible or irreversible attachment of enzymes on a support, which is then coated with cationic polymers (i.e., polyethyleneimine-PEI, polyallylamine-PAH) for the ionic adsorption of the cofactors on the same support (i.e., porous materials).[11-13] Such electrostatic interactions occur between the positively charged amine moieties of the polymeric coating and the negatively charged phosphate groups of phosphorylated cofactors (i.e., NAD(P)H, PLP, FAD). Through multidimensional kinetic and thermodynamic analysis, our group has revealed the essence of an association/dissociation equilibrium that occurs within the ssHBs under operating conditions, enabling the cofactors to travel from the surface of the support to the active site of the immobilized enzymes without lixiviating.[13] In-depth understanding of the interactions between the cofactors and the support as well as their interplay with the co-immobilized enzyme, has allowed us to design a battery of ssHBs that are yet limited to biotransformations that operate under low ionic strength conditions (**Scheme 1a**). Under high ionic strength, the cofactors lixiviate and thus the heterogeneous biocatalyst is no longer self-sufficient, preventing the reusability of both the cofactor and the enzyme. However, several enzymatic reactions require the use of high ionic strength either due to the need for high buffer concentration for pH and/or enzyme stability or due to the saline nature of some of the substrates (i.e., ammonium formate). This is the case of an ssHB that co-immobilizes a transaminase and a reductase together with NADH and PLP for the synthesis of L-pipecolic acid.[14] In such case, a high buffer concentration is required to maintain stable the activity of the reductase, so the electrostatically adsorbed cofactors lixiviate and the continuous operation of the ssHB is precluded without their exogenous supply. Likewise, ssHBs based on electrostatic interactions fail to synthesize L-Alanine without the exogenous addition of NADH because this biotransformation requires a high concentration of ammonium formate as a co-substrate.[15] Furthermore, these ssHBs would also function inefficiently for other industrially relevant biotransformations, such as the reductive amination of ketones and aldehydes that are catalyzed by amine dehydrogenases which demand high concentrations of ammonium buffer,[16-20] and the intensification of bioredox cascades that rely on phosphite dehydrogenases for the recycling of NAD(P)H.[21]

Reversible covalent bonding may prevent unwanted cofactor lixiviation in the presence of high ionic strength while maintaining an optimum cofactor association/dissociation equilibrium. In addition to the phosphate groups displayed in the nucleotide skeleton of adenylated cofactors (i.e., NAD(P)H, NAD^+, ATP) they also display ribose molecules which can act as potential covalent bond acceptors. Boronic acids are well-known molecules that form esters driven through H-bonding with *cis*-diol moieties, including sugars like ribose, which is one of the strongest reversible interactions in an aqueous solution.[22, 23] In fact, the complexation of ribose groups of adenylated cofactors with boronic acids, has been specifically explored in solution through electrospray ionization, mass spectrometry (ESI-MS), and nuclear magnetic resonance (NMR) spectroscopy.[24-26] These studies directly investigate the esterification of

boric acid and borate to carbohydrates proving that complexation is occurring through the *cis*-2,3-ribose diol of the cofactors rather than through their phosphate group.

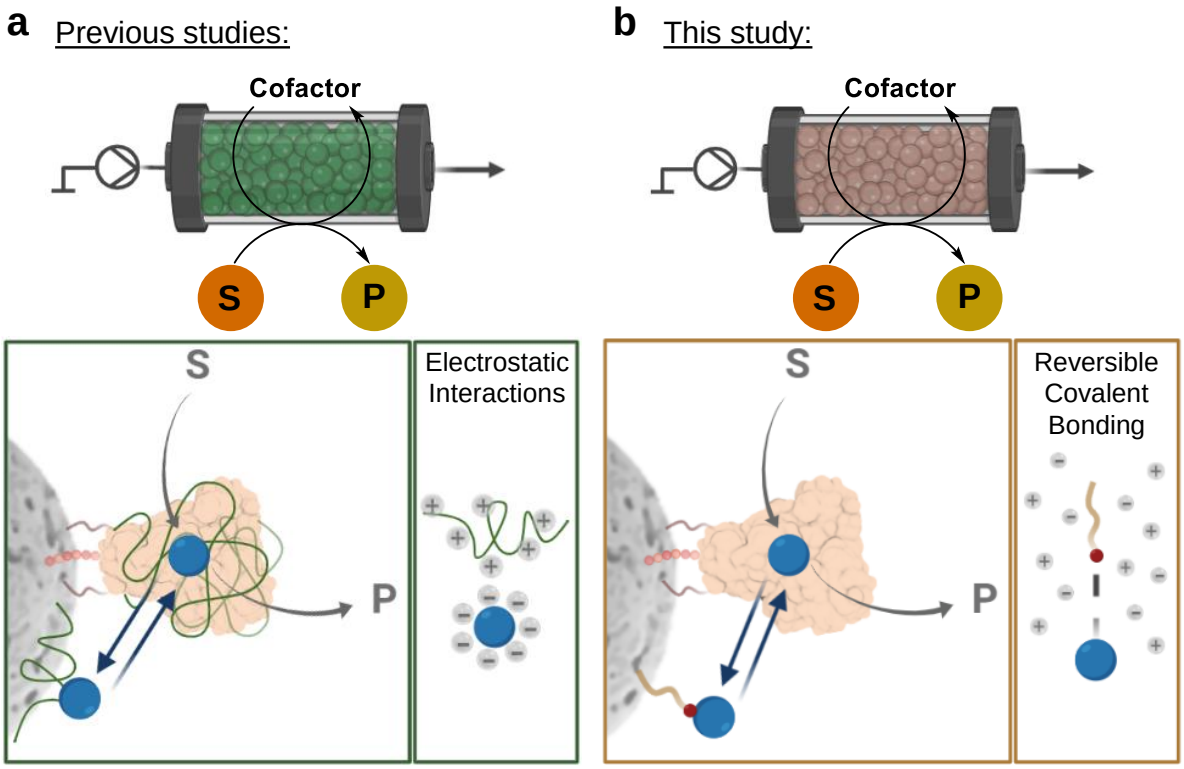

Scheme 1. Schematic illustration of cofactor regeneration in self-sufficient heterogeneous biocatalysis systems where the cofactor co-immobilization occurs either **a)** through electrostatic interactions (previous studies)[4, 6, 8], or **b)** through reversible covalent bonding (this study). S: substrate, P: product. The cofactor is represented as a blue sphere.

Despite the mature concept of boron-adenylated cofactor complexation that has been applied for a diversity of configurations,[27-29] examples of cofactor immobilization through boronic acid adduction are scarce in biocatalysis. Wilner and co-workers have pioneered the use of this chemistry to co-immobilize enzymes with their corresponding adenylated cofactors. [29, 30] They demonstrated that the cofactor is available to the entrapped enzymes but no reuse of the cofactor or the enzymes was reported under any conditions. Furthermore, the nature of the interactions that govern the complexation between the adenylated cofactor and the boronic acid when anchored to the support was not explored. Therefore, the potential and the scope of boronic acid-diol adducts to fabricate ssHBs that withstand high ionic strength remain unexplored.

In this work, we integrate this specific complexation chemistry into the fabrication of ssHBs capable of working under high ionic strength reaction conditions (**Scheme 1b**). To do so, we leveraged our experience in the development of heterofunctional supports[8, 12, 31] to co-immobilize several adenylated cofactors with selected cofactor-dependent enzymes on agarose porous microbeads functionalized with both phenyl boronic acid and cobalt-chelates. We characterized the molecular basis that rules the interaction between adenylated cofactors and supported boronic acids through different spectroscopic techniques, confirming that the ribose motif of the cofactors drives the interaction to form boron esters. The resulting ssHBs operate under high ionic strength conditions with negligible lixiviation of the bound cofactors,

enabling reductive amination reactions without exogenous cofactor addition both in batch (discontinuous) and in flow (continuous) reactors.

RESULTS AND DISCUSSION

Functionalization of cobalt-chelates activated agarose microbeads with boronic acid and their capability to immobilize His-tagged enzymes and adenylated cofactors. First, we prepared a new heterofunctional support containing cobalt-chelates (Co^{2+}) and aryl boronic acid as ligands to immobilize His-tagged enzymes and adenylated cofactors, respectively (**Figure 1a**). Further experimental details to prepare these heterofunctional supports can be found in the section *Materials and Methods*. The density of cobalt-chelates and boronic groups was optimized and characterized by ultraviolet–visible (UV-Vis) spectrophotometry and X-ray photoelectron spectroscopy (XPS) (**Figure S1 and S2**) which confirmed that both Co(II) and boron atoms were bound to the surface of the agarose microbeads. Magic angle spinning nuclear magnetic resonance (MAS-NMR) spectroscopy shows that the immobilized aryl boronic acid (3-APBA) presents a single broad peak at 18.5 ppm unlike its free counterpart, which has a quadrupolar coupling constant, C_Q = 3.15 MHz, quadrupolar asymmetry parameter, $|_Q$ = 0.4, and isotropic chemical shift, δ_{iso} = 28 ppm (**Figure 1b**).[32] The loss of the quadrupolar interaction indicates that the boron atom of the aryl boronic presents a pseudo-sp^3 hybridization. The neutral conditions of the immobilization avoid the formation of borate species ($ArB(OH)_3^-$), thus suggesting an intermolecular interaction with hydroxyl groups of the agarose structure (**Figure 1a**).

After the preparation of AG-B/Co^{2+} support, we co-immobilized His-tagged enzymes and adenylated cofactors through cobalt-histidine coordination bonds and boronic acid-ribose covalent bonds, respectively (**Figure 1a**). For this study, we selected three different His-tagged enzymes whose activities depend on adenylated cofactors; NAD(P)H-dependent alcohol dehydrogenase from *Bacillus stearothermophilus* (ADH), NADH-dependent L-Alanine dehydrogenase from *Bacillus subtillis* (AlaDH), NAD^+-dependent formate dehydrogenase from *Candida boidinii* (FDH), NAD(P)H-dependent β-aminoacid dehydrogenase from *Candidatus Cloacimonas acidaminovorans* (AmDH) and $NAD(P)^+$-dependent ketoreductase from *Lactobacillus kefir* (KRED). The assayed enzymes reach 100% of immobilization yield despite the low Co^{2+} density (2.3 μmol g^{-1}) as displayed for each selected support (**Table 1**). Once the enzymes were immobilized, we optimized the immobilization of several adenylated cofactors using NADH as a model.

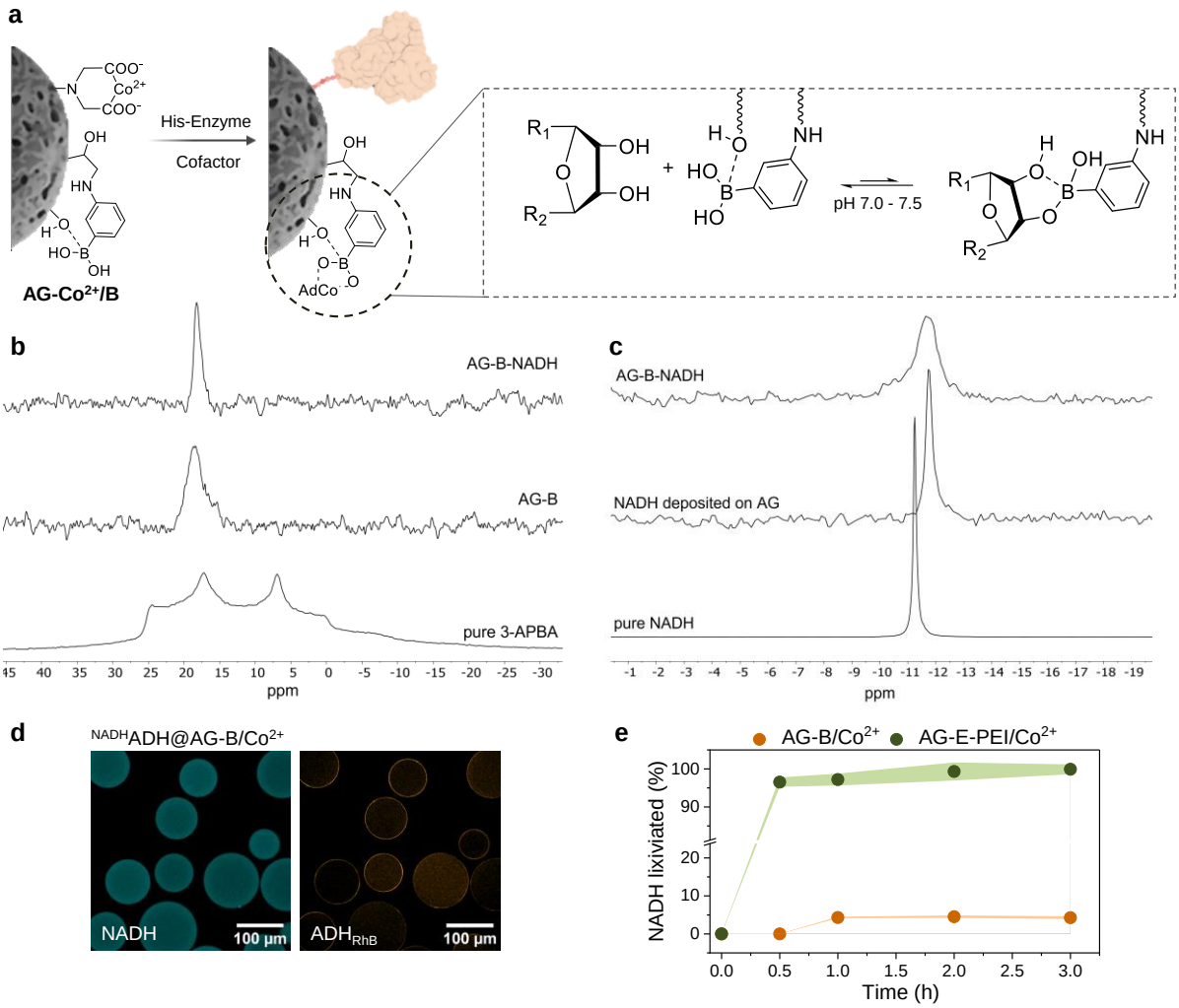

Figure 1. a) Surface chemistry of porous agarose microbeads (AG-B/Co^{2+}) and the reversible boronic acid-diol complexation that drives the co-immobilization of adenylated cofactors (AdCo) with the His-tagged enzymes on this support. **b)** ^{11}B MAS-NMR spectra of pure 3-APBA, AG-B, and AG-B-NADH, **c)** ^{31}P MAS-NMR spectra of pure NADH, NADH deposited on unmodified AG and AG-B-NADH. **d)** Confocal fluorescence microscopy presenting the spatial organization of the fluorescent adenylated cofactor, NADH (blue channel, λ_{ex}: 405 nm), and the RhB labeled ADH (red channel, λ_{ex}: 561 nm) inside the AG-B/Co^{2+} supports. **e)** Lixiviated concentration (%) of NADH bound on AG-B/Co^{2+}-ADH and AG-E/Co^{2+}-ADH coated with PEI, after 3 hours of incubation in Tris-HCl 10 mM and NaCl 1 M at pH 7. AdCo: Adenylated cofactor.

Hence, we tested the cofactor immobilization efficiency under different conditions: cofactor concentration, incubation time, pH, buffer, and ionic strength (**Table S1**). Our criterium for optimum cofactor binding conditions was the maximum loading of cofactor per mass of support at the shortest incubation time to minimize the cofactor degradation during immobilization.[33] Accordingly, the optimal binding conditions for NADH were 3 hours of incubation of 10 mM NADH in 100 mM Tris-HCl at pH 7 and 25 ºC, resulting in loading concentrations of ~17 µmol g^{-1} on AG-B/Co^{2+} supports. Final optimal immobilization conditions were also applied for the binding of other adenylated cofactors (NADPH, $NADP^+$, NAD^+, FAD, and ATP) to AG-B/Co^{2+} supports (**Table S1**).

Table 1. Immobilization parameters of the enzymes immobilized on AG-B/Co^{2+} support for subsequent activity studies. All parameters were obtained as described in the section of *Materials and Methods*.

Support	Biocatalyst	Enzyme	Ψ	Enzyme Load	Cofactor	Cofactor load
			%	mg $g^{-1}_{support}$		µmol g^{-1}
AG-B/Co^{2+}		ADH	100	1	NADH	15[a]
AG-B/Co^{2+}		AlaDH	100	0.07	NADH	5.6[b]
AG-B/Co^{2+}		FDH	100	3	NAD^+	8.3[b]
AG-B/Co^{2+}	$ssHB(B)_1$	AlaDH | FDH	100 | 80	2 | 10	NADH	15[a]
AG-PEI/Co^{2+}	$ssHB(PEI)_1$		100 | 60	2 | 6	NADH	17[a]
AG-B/Co^{2+}	$ssHB(B)_2$	AmDH | KRED	100 | 100	10 | 5	NADPH	17[a]
AG-PAH/Co^{2+}	$ssHB(PAH)_3$	ATA	50	3.6	PLP	9.8[b]

[a] Offered [NAD(P)H] 100 µmol g^{-1}, [b] Offered [NADH] 10 µmol g^{-1}
For details of the immobilization parameters, Immobilization yield (Ψ) and Cofactor load see in Materials and Methods in the sections of *Enzyme immobilization and co-immobilization* and *Cofactor immobilization and lixiviation studies*, respectively.

The presence of NADH on the surface of the AG-B/Co^{2+} was confirmed by XPS (**Figure S3**) and MAS-NMR measurements (**Figure 1b-c**). ^{31}P MAS-NMR spectra show that the chemical shifts of the bound NADH (11.2 ppm) and the free counterpart (11.7 ppm) are identical, but the signal is significantly broadened upon immobilization (**Figure 1c**). This wider NMR signal suggests that NADH mobility is greatly reduced. When we soaked plain agarose (without 3-APBA) with NADH, the ^{31}P signal of NADH is much narrower, supporting the key role of 3-APBA in the immobilization of NADH. Furthermore, we observed that the ^{11}B signal of immobilized 3-APBA was narrower upon its incubation with NADH (**Figure 1b**). This narrower signal suggests that the ribose of NADH replaces the hydroxyl groups of the agarose to form a more stable tetrahedral boron-cis-diol adduct, making the boron atom more mobile but maintaining its pseudo-sp^3 hybridization (**Figure 1a**). Therefore, the mobility changes found in boron and phosphate atoms of the immobilized aryl boronic and NADH molecules, respectively, support the existence of a supramolecular interaction between them. Hence, we suggest that such interaction is based on covalent bonding between the boronic acid and the ribose of NADH forming a reversible boronate ester, discarding a direct interaction with the cofactor phosphates.

Next, we studied the binding thermodynamics of different cofactor/enzyme pairs under steady-state batch conditions (**Figure S4**). Langmuir adsorption isotherms show that NADH, NAD^+, and FAD adsorb differently, but reversibly, on the AG-B/Co^{2+} supports. From the Langmuir isotherms, we calculated the dissociation constants (K_D) for each adenylated cofactor, obtaining similar values for NADH (K_D = 0.5 ± 0.1 mM) and NAD^+ (K_D = 0.2 ± 0.03 mM). Similar binding affinities of both reduced and oxidized nicotinamide cofactors to AG-B/Co^{2+} can be explained because their common ribose groups are driving their immobilization. Interestingly, the K_D of NADH herein determined falls in the same order of magnitude as K_D of NADH adsorbed on PEI-coated microbeads through electrostatic interactions (K_D = 0.2 ± 0.02 mM), which makes this interaction suitable to allow the reversibly bound cofactors traveling to the active sites of the immobilized enzymes.[13] In contrast, FAD shows twice higher K_D = 1.0 ± 0.9 mM than NADH, suggesting that the two ribose units of the nicotinamide cofactor promote a stronger binding than the flavin cofactor which only has one unit. Remarkably, such a

difference is not observed when both FAD and NADH are electrostatically bound to support functionalized with PEI through phosphate-amine ionic bonds, supporting the fact that ribose is driving the interaction between the adenylated cofactors and the agarose functionalized with boronic groups.

As we propose that the interaction of adenylated cofactors (i.e., NADH) and supported boronic acids is governed by covalent bonding rather than electrostatic interactions, we incubated the immobilized NADH on AG-B/Co^{2+} with high ionic strength conditions to test whether NADH-boronic acid complexation resists high concentrations of salt. To do so, we fabricated a model heterogeneous biocatalyst where ADH was co-immobilized with NADH on AG-B/Co^{2+} supports (**Table 1**, ^{NADH}ADH@AG-B/Co^{2+}). Harnessing the autofluorescence properties of NADH, we initially performed fluorescence microscopy imaging to visualize its binding on AG-B/Co^{2+} supports (**Figure S5a**) as well as confocal laser scanning microscopy imaging (CLSM) to explore its spatial organization on the AG-B/Co^{2+} support (**Figure S5b**). Fluorescence images reveal a uniform distribution of NADH throughout the whole porous surface of AG-B/Co^{2+}. Subsequently, we performed CLSM imaging on the co-immobilized system (**Figure 1d**) which reveals that NADH only colocalizes with the Rhodamine B (RhB) labeled ADH at the outer surface of the support where ADH is mostly immobilized. For the lixiviation studies, we incubated the ssHB for 3 hours in 10 mM Tris-HCl and 1 M NaCl, at pH 7 (for more experimental details see *Materials and Methods*). As a sample reference, we co-immobilized ADH and NADH on supports where the latter was immobilized through electrostatic interactions. For that, we used epoxy-activated agarose (AG-E) microbeads activated with cobalt-chelates for the site-directed immobilization of ADH and then we coated the biocatalyst with PEI (AG-PEI/Co^{2+}) to ionically adsorb NADH. As NADH presents similar K_D values when immobilized on the two systems, we loaded similar NADH concentrations on both supports (3.5 μmol g^{-1}) for lixiviation studies. **Figure 1e** shows that NADH is minimally released (4.5%) to the bulk after 3 h of incubation when immobilized on AG-B/Co^{2+}, whereas electrostatically bound NADH on AG-PEI/Co^{2+} is quantitatively lixiviated (>99%) after the first 30 min. This fact is supported by single-particle studies where NADH remains inside the AG-B/Co^{2+} microbeads but it lixiviates from the inner surface of the AG-PEI/Co^{2+} microbeads (**Figure S6**). The lixiviation together with NMR spectroscopy studies, in agreement with literature reports, [22-26] demonstrate that the *cis*-2,3 diols of the ribose units of NADH interact with the supported boronic acid forming covalent bonds (boronate esters) rather than electrostatic interactions.

Single-particle kinetic studies of the self-sufficient heterogeneous biocatalysts. To understand the functionality of the immobilized enzymes towards their confined adenylated cofactors under high ionic strength conditions, we co-immobilized different enzyme/cofactor pairs. **Table 1** compiles the immobilization parameters of mono and bi-enzymatic systems co-immobilized on AG-B/Co^{2+} with their corresponding nicotinamide cofactors. In all cases, the immobilized enzymes were active, and the cofactors were successfully immobilized, while depending on the investigated system the enzyme/cofactor ratio varies (**Table 1**). To demonstrate that the cofactor molecules are still available for the immobilized enzymes when complexed with boronic acid, we performed a single-particle analysis which inform us about the intraparticle kinetics of ssHBs, as well as about the particle-to-particle functional heterogeneity.[13] Detailed conditions of the single-particle assays are described in the section of *Materials and Methods*. We initially determined the intraparticle specific activity of ADH co-immobilized with NADH either on AG-B/Co^{2+} or AG-PEI/Co^{2+} under low (w/o NaCl) and high ionic strength (NaCl 1 M) (**Figure 2a**).

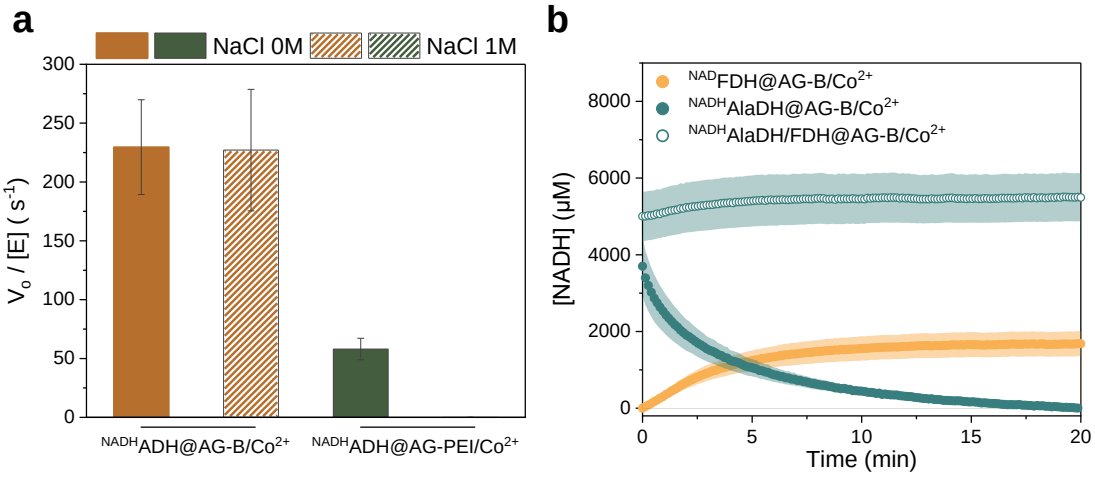

Figure 2. a) Bar plot of ADH specific activity determined by single-particle kinetic studies using ADH immobilized on AG-B-NADH/Co^{2+} (orange) and AG-PEI-NADH/Co^{2+} (green) supports before and after the addition of 1 M NaCl. The initial rate (V_0) is defined as the concentration of cofactor consumed per second. **b)** Single-particle time-courses of NADH oxidation and NAD^+ reduction in the presence of 0.5 M ammonium formate and 75 mM pyruvate in 0.1 M potassium phosphate buffer pH 8 using single immobilized and co-immobilized AlaDH and FDH systems (ssHB$(B)_1$) on AG-B/Co^{2+} supports. Time data points are obtained from the mean value of 25 microbeads (50 – 150 μm) with the standard deviation depicted in shadows of the same color.

Interestingly, the specific activity of ADH co-immobilized with NADH on AG-B/Co^{2+} is negligibly affected by the presence of high salt concentrations during the reduction of acetone (**Figure 2a**), unlike the soluble enzyme whose activity decreases 46 % at 1 M NaCl (**Figure S7**). On the other hand, when ADH is co-immobilized with NADH on AG-E-PEI/Co^{2+} fully loses its activity under high ionic strength conditions (NaCl 1M). This dramatic inactivation of ADH immobilized on AG-E-PEI/Co^{2+} is linked to the lixiviation of NADH from the microbeads, which provokes the dilution of the cofactor into the bulk, thus the decrease of the local NADH concentration in the surroundings of the immobilized enzyme (**Figure 2a**). Even under low ionic strength conditions, we find a 5-fold higher specific activity of the immobilized ADH when the cofactor is complexed with boronic acid than when it is electrostatically bound to the PEI coating. This impaired enzyme activity hints at inhibition/inactivation of the enzyme activity when it is coated with PEI which.

To evaluate this strategy with other adenylated cofactors, free hexokinase, and glucose-6-phosphate dehydrogenase were mixed with ATP and $NADP^+$ co-immobilized on AG-B/Co^{2+} through ribose-boronic acid complexation (**Table S1**). In this reaction sequence, the hexokinase phosphorylates glucose to glucose-6-phosphate at the expense of ATP, followed by the glucose 6-phosphate oxidation catalyzed by the glucose-6-phosphate dehydrogenase that concomitantly reduces $NADP^+$ to NADPH (**Figure S8a**). The throughput of this cascade was assessed through spectrophotometric measurements of the amount of NADPH produced in the presence of glucose. The throughput of this bi-enzyme cascade using co-immobilized ATP and $NADP^+$ on AG-B/Co^{2+} increases at 300% in comparison to the free system (both enzymes and cofactor in solution) (**Figure S8b**). These differences in reaction kinetics arise on the fact that the local concentration of both cofactor within the agarose pores are higher than in solution, thus increasing the activity of the bi-enzymatic system freely diffusing through the porous surface. Hence, immobilizing both ATP and NADPH enables a superior cascade throughput even with lower amounts of $NADP^+$ (18 nmoles) than in solution (200 nmoles).

Encouraged by the negligible cofactor lixiviation, as well as by the high specific activity under high ionic strength, we fabricated a new set of ssHBs that require high excess of ammonium formate as amino and electron donor to achieve the synthesis of L-α-amino acids[15]. To this end, we co-immobilized AlaDH and FDH dehydrogenases (system 1) for the reductive amination of pyruvate to L-Alanine. In this reaction, AlaDH requires NADH as a redox cofactor and ammonium formate as the amino donor. In parallel, FDH regenerates the NADH pool *in situ* due to the oxidation of formate into carbon dioxide.[34-36] Detailed conditions of co-immobilization of both enzymes, as well as their separate immobilization on AG-B/Co2+ supports, are described in *Materials and Methods*. In the past, our group investigated the synthesis of enantiopure L-α-amino acids catalyzed by co-immobilized AlaDH and FDH in both batch and flow reactors using an exogenous supply of NADH.[15] In the present study we aim to reproduce that bi-enzyme system but introduce the co-immobilization of NADH together with the enzymes on the same microparticles to work as a self-sufficient heterogeneous biocatalyst (**Table 1**, ssHB$(B)_1$). Hence our challenge is to prevent the cofactor lixiviation in the presence of the high concentration of ammonium formate required for the enzyme cascade. We first co-immobilized AlaDH and FDH sequentially, through metal coordination and NADH through H-bonding on AG-B/Co^{2+} microbeads. As control samples, we co-immobilized each enzyme separately with their corresponding adenylated cofactor; NADH for AlaDH and NAD^+ for FDH (**Table 1**). Through single-particle experiments, we can monitor the intraparticle NADH concentration over time. When AlaDH or FDH are immobilized separately, they either consume or produce NADH, which is associated with the respective increase or decrease of the NADH fluorescence, respectively. Single-particle studies confirm that the NADH co-immobilized with AlaDH is oxidized to NAD^+ within the beads in the presence of pyruvate and ammonium (**Figure 2b**). Likewise, the NAD^+ co-immobilized with FDH is reduced to NADH using formate as substrate (**Figure 2b**). In contrast, when both enzymes were co-immobilized on the same microbead, the intraparticle NADH concentration remains constant (**Figure 2b**). These results evidence the efficient intraparticle recycling of NADH in the presence of high ionic strength (0.5 M ammonium formate and 75 mM pyruvate in 0.1 M potassium phosphate buffer pH 8). Hence NADH does not lixiviate while it travels from one enzyme to the other within the pores of the microbead (**Figure S9**). Control experiments with no immobilized enzymes show a negligible fluorescence drift over time, therefore changes in volumetric fluorescence intensity are the result of biocatalytic activities (**Figure S10**) (for more details see *Materials and Methods*).

Utilizing the data set we obtained during the time-lapse fluorescence experiments at the single-particle level, we explored the particle-to-particle functional variability of ^{NAD}FDH@AG-B/Co^{2+} and ^{NADH}AlaDH@AG-B/Co^{2+}. We first observe a negative correlation of the initial rate (V_o) with the particle radius for both AlaDH and FDH (**Figure S11a**). This trend agrees with our recent findings[13] and is attributed to the particle size heterogeneity (50 – 150 μm), as the immobilized cofactor concentration varies depending on the size of the microbeads (**Figure 11b).**

Reductive aminations catalyzed by self-sufficient heterogeneous biocatalysts. Once the functionality of ssHB$(B)_1$ (loading AlaDH, FDH, and NADH), was characterized, we utilized it for the synthesis of L-Alanine (**Figure 3a**) in batch-mode. Initially, we compared the reaction course when NADH is co-immobilized (bonded to boronic acid) and when is exogenously supplemented keeping the same concentration of NADH per mass of support (17 μmol g^{-1},

Table 1). Both systems catalyze the reductive amination of 75 mM pyruvate, reaching a product chromatographic yield of 33% after 4 hours.

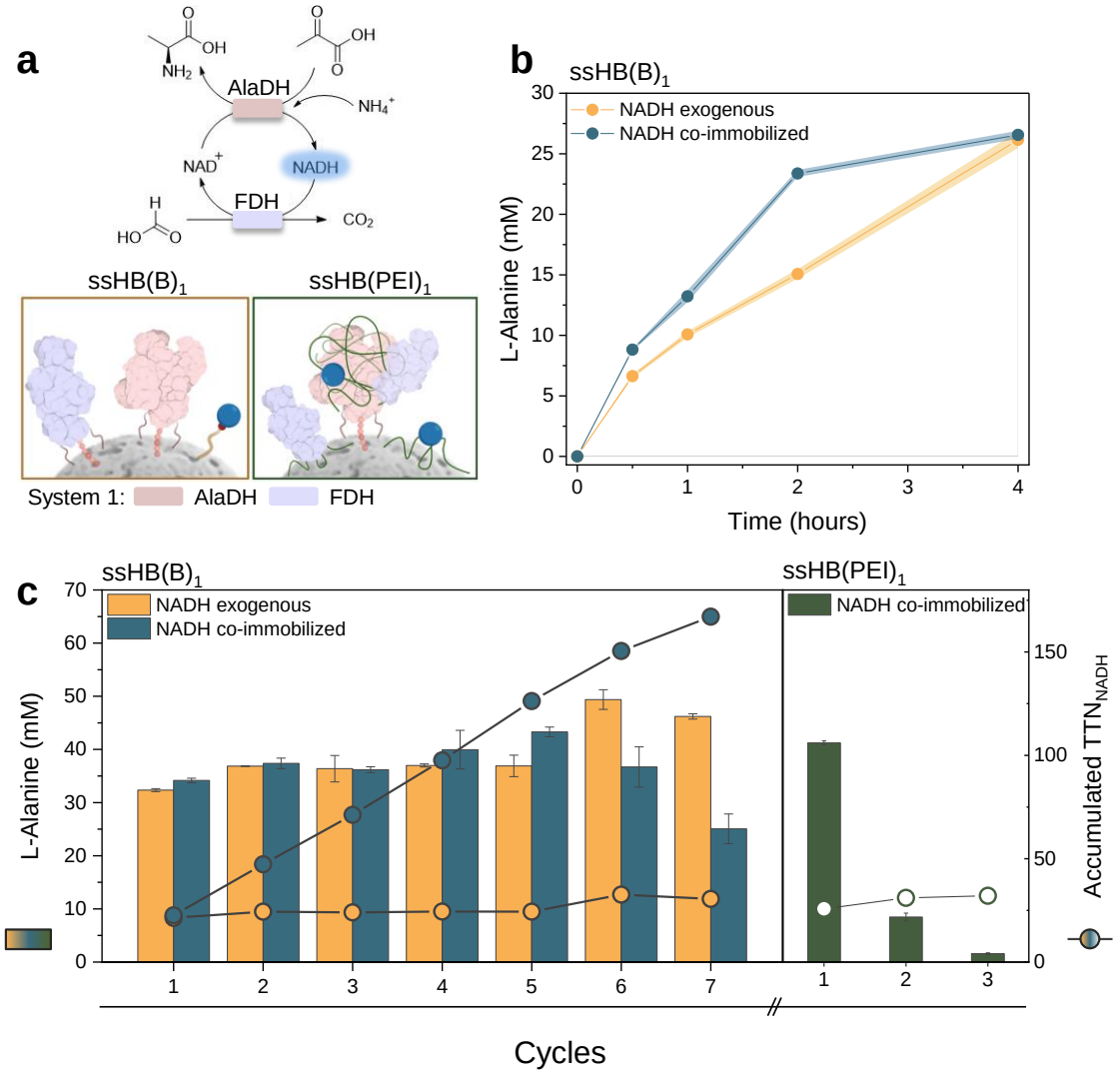

Figure 3. a) Reaction scheme of L-Alanine biosynthesis integrating the *in situ* cofactor regeneration catalyzed by AlaDH and FDH (system 1) and schematic illustration of two bi-enzyme self-sufficient heterogeneous biocatalysts where the cofactor is bonded through covalent (ssBH(B)$_1$) and ionic bonds (ssBH(PEI)$_1$). **b)** Reaction courses of L-Alanine synthesis catalyzed by ssHB(B)$_1$ with (yellow line) and without (blue line) exogenous supply of NADH. **c)** Reuse in batch-mode of ssBH(B)$_1$ (15 μmol NADH g^{-1}) and ssBH(PEI)$_1$ (17 μmol NADH g^{-1}) for the synthesis of L-Alanine (left y-axis) and the corresponding accumulated TTN of NADH after 4-hours cycles (right axis). Biocatalysts were washed three times after each cycle with 10 mM potassium phosphate buffer at pH 8. The reaction mixture in experiments presented in panels b and c consisted of 0.5 M ammonium formate, 75 mM pyruvate, and 1.5 mM NADH (when NADH is exogenous) in 0.1 M potassium phosphate buffer at pH 8 and 25 ºC.

Nevertheless, when NADH is exogenously added, the biotransformation occurs 2.3 times slower than only using ssHB(B)$_1$ according to the first-order kinetic constant of the reaction courses (**Figure 3b and S12**), which means volumetric productivity of 0.58 g L^{-1} h^{-1}. The higher operation effectiveness of ssHB(B)1 compared to the system using exogenous cofactor may be due to the greater local NADH concentration when co-immobilized with the enzyme (15 μmol g^{-1} ≈ 10 mM inside the bead) compared to the 1.5 mM NADH exogenously diluted in the bulk.

More importantly, ssHB(B)$_1$ yields similar titers of L-Alanine (~38 ± 3.2 mM) in 6 consecutive batch cycles (each cycle: 4 hours) like the system supplied with exogenous NADH after each cycle (**Figure 3c**). L-alanine is stably produced during consecutive batch cycles in which NADH is neither leached nor the enzyme is inactivated during discontinuous use of this ssHB. Remarkably, immobilized AlaDH and NADH reach an accumulated total turnover number (TTN)[37] of 3.5 x 10^5 and 167, respectively, after 6 consecutive reaction cycles, while the TTN of the exogenous NADH was only 26 ± 4, as a fresh cofactor is added after each cycle. In contrast, **Figure 3c** also shows a considerable reduction of the operational stability when the cofactor is immobilized through electrostatic interactions with the PEI coating (ssHB(PEI)$_1$, (**Figure 3a**). The L-Alanine titer decreases 25 times after the third batch cycle (from 41 mM to 1.6 mM), indicating that the immobilized NADH is lixiviated under 0.5 M ammonium formate, in agreement with the results observed in **Figure 2a**. Finally, to further explore the effect of NADH load on the operational stability of our system, we performed a 30 min batch cycle of the L-Alanine synthesis using ssHB(B)$_1$ which loads different concentrations of NADH: 0.3 μmol g^{-1}, 1.3 μmol g^{-1} and 17 μmol g^{-1} (**Figure S13a**). The volumetric activity of the ssHB(B)$_1$ loaded with 17 μmol_{NADH} g^{-1} is 9 times higher than the same biocatalyst loaded with 0.3 μmol_{NADH} g^{-1}. We suggest that the lower productivity of the biocatalyst is mainly due to the lower NADH local concentration available for the immobilized enzymes. Furthermore, the operational stability is also maximized when the ssHB(B)$_1$ is loaded with 17 μmol_{NADH} g^{-1} (**Figure S13b**).

To expand the application scope of the developed cofactor immobilization chemistry on AG-B, we designed ssHB(B)$_2$ which is capable to transform the acetoacetic acid into 4-aminobutyrate. In this system, an NADPH-dependent β-amino acid dehydrogenase (AmDH) utilizes a high concentration of ammonium chloride (500 mM) as an ammonia source and is coupled to a cofactor regeneration system ($NADP^+$ to NADPH) comprised of a ketoreductase (KRED) that concomitantly transforms isopropanol into acetone (system 2, **Figure S14a**). Both AmDH (10 mg g^{-1} of support) and KRED (5 mg g^{-1} of support) were co-immobilized sequentially by cobalt-histidine coordination bonds, and NADPH through boronic acid-ribose covalent bonding (**Table 1**). Enzyme immobilization reached 100% yield in both cases after one hour of incubation, and recovered activities were 23 and 79% for AmDH and KRED, respectively. With the assembled enzymes, we tested the NADPH immobilization in the best conditions found for NADH (3 hours of incubation of 10 mM NAPDH in 100 mM Tris-HCl pH 7 at 25 ºC). As a result, we reached similar immobilization titters as in the ssHB(B)$_1$, (17 μmol g^{-1}, Table 1). This fully assembled self-sufficient heterogeneous biocatalyst (ssHB(B)$_2$) was tested in the amination of lithium acetoacetate and compared with its soluble counterpart. Both immobilized and free systems exhibited a similar performance for the reductive amination cascade. The reaction rate was particularly slow due to the low specific activity of AmDH towards this substrate (≈ 6 mU mg^{-1}), producing 3.14 and 3.98 mM of aminobutyrate in a period of 48 hours when using ssHB(B)$_2$ and the soluble enzymes, respectively. Further analysis revealed an exquisite AmDH enantioselectivity, achieving >99% enantiomeric excess of the *S*-enantiomer in both cases (**Figure S14b**). Although reaction yields are low, ssHB(B)$_2$ manages to recycle each molecule of immobilized NADPH 2 times (**Figure S14c**), confirming the reuse of the covalently immobilized cofactor.

Reductive aminations catalyzed by self-sufficient heterogeneous biocatalysts in continuous flow mode. The operational stability of the ssHB(B)$_1$ encouraged us to integrate this biocatalyst into flow reactors for the continuous synthesis of L-Alanine. We packed 900

mg of ssHB(B)$_1$ into a plug-flow column at a flow rate of 25 µL min^{-1} (for more details see *Materials and Methods*). Initially, we fed this packed bed reactor (PBR) with 50 mM ammonium formate and 7.5 mM pyruvate in 0.1 M potassium phosphate buffer at pH 8 and 25 ºC. Under these conditions, ssHB(B)$_1$ works under lower ionic stress than under the conditions explored in the batch-mode reaction (**Figure 4a**). At lower substrate loads and ionic strength, a 99% chromatographic yield of L-Alanine is achieved with a space-time-yield (STY) of 0.62 g L^{-1} h^{-1}, the product titer is stable for 24 hours of continuous operation, and the accumulated TTN$_{NADH}$ is 20.

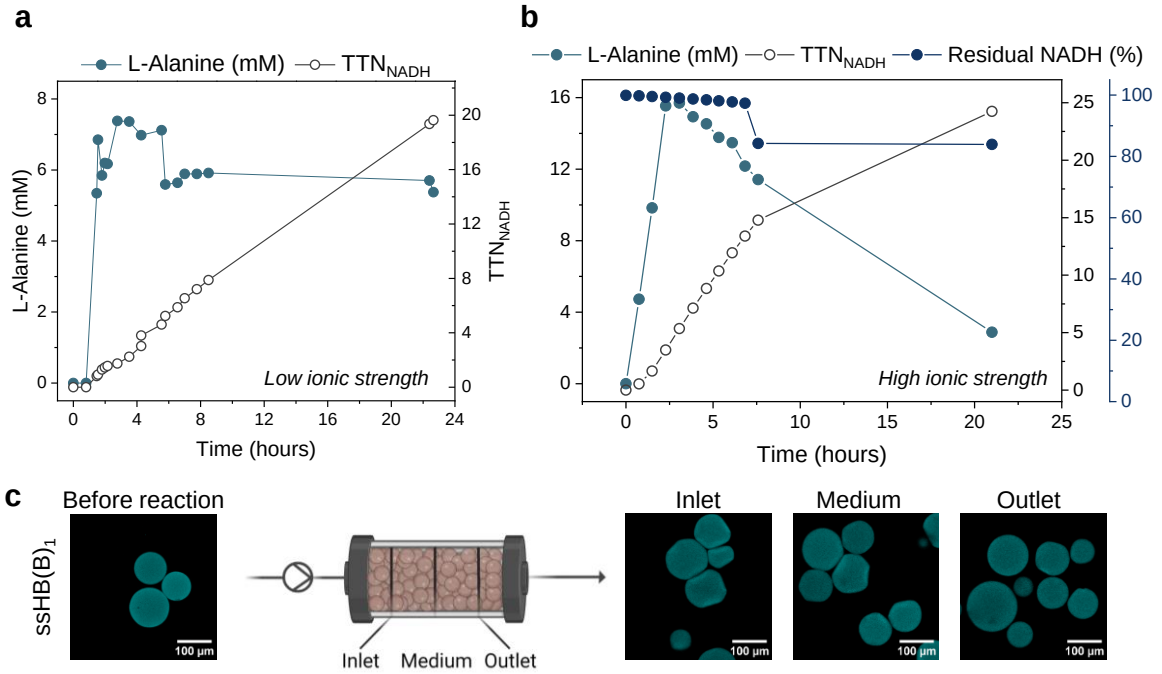

Figure 4. Continuous synthesis of L-Alanine in a PBR loaded with ssHB(B)$_1$. The reactor was fed with **a)** 50 mM ammonium formate, 7.5 mM pyruvate, and **b)** 0.5 M ammonium formate, 75 mM pyruvate in 0.1 M potassium phosphate buffer at pH 8 and operated at a flow rate of 25 µL min-1 at 25 ºC. The left y-axis represents the L-Alanine titer, and the right y-axis shows the accumulated TTN of NADH. The second right y-axis in panel b represents the residual immobilized NADH (blue color) at each time point. **c)** *Ex-situ* evaluation of the NADH bound ssHB(B)$_1$ after 21 hours of continuous operation using 0.5 M ammonium formate, and 75 mM pyruvate in 0.1 M potassium phosphate buffer at pH 8. Confocal fluorescent images (blue channel, λ_{ex}: 405 nm) of the microbeads of the ssHB(B)$_1$ before reaction in flow and extracted from the inlet, medium, and outlet sections of the PBR upon 24 h of continuous operation.

Subsequently, the same PBR is fed with 0.5 M ammonium formate, and 75 mM pyruvate in 0.1 M potassium phosphate buffer at pH 8 and 25 ºC under the same flow rate. Under these conditions, the system reaches a maximum steady state L-Alanine titer of 17 mM (23 % yield) after 2 hours of operation, which means a STY = 2.2 g L^{-1} h^{-1}; a value roughly two times higher than the volumetric activity of the batch reactor under the same conditions. The STY value is similar to that reported, for other reductive amination cascades in flow but using exogeneous supply of cofactor.[19, 20] Unfortunately, the maximum titer and the STY of ssHB(B)$_1$ gradual decay to 3.4 mM and 0.30 g x L^{-1} h^{-1}, respectively, after 21 hours (**Figure 4b**). Despite this operational inactivation, the ssHB(B)$_1$ presents an accumulated TTN$_{NADH}$ of 25 after 21 hours. This value is significantly lower than the one achieved with the same biocatalysts but operated

in a discontinuous batch mode. Although immobilized NAD(P)H can be recycled to a higher extent using other versions of self-sufficient heterogeneous biocatalysis under continuous operations under low ionic strength,[38] this is the first time that the proposed chemistry is used to create self-sufficient heterogeneous biocatalysts operating effectively under elevated ionic strength conditions. The concept of immobilized NAD(P)H for reductive amination reactions in such conditions has potential for further advancements and refinements in our technology.

To investigate the reasons behind the limited TTNs of the PBR due to the decrease of the STY over time, we quantified the residual co-immobilized NADH by measuring the absorbance (340 nm) of the flow through solutions during the continuous operation. **Figure 4b** shows that 80% of the initial loaded NADH remains bound to the heterogeneous biocatalyst as negligible leaking was observed during the process. Furthermore, we recovered the microbeads from different longitudinal sections of the PBR (inlet, medium, or outlet) after its operation and performed *ex-situ* confocal fluorescence imaging to explore differences in the intraparticle NADH concentration. **Figure 4c** shows a similar NADH intraparticle fluorescence of exhausted microbeads as their fresh counterpart regardless of the PBR section, supporting the fact that the cofactor remains inside the support. According to these experimental data, we ruled out NADH lixiviation to explain the inactivation of ssHB(B)$_1$ during continued use. Alternatively, enzyme lixiviation may explain the operational inactivation of this heterogeneous biocatalyst. However, we found negligible enzyme lixiviation from the microbeads collected from the different sections of the PBR as shown in the SDS-PAGE gel (**Figure S15a**). Finally, we tested the remained activity of the immobilized enzymes after their continuous operation in the PBR. We observed that both AlaDH and FDH lost 85 and 90% of their initial activity, respectively, after working for 30 hours in flow (**Figure S15b**). Therefore, the performance of the ssHB(B)$_1$ is deteriorated by the intrinsic enzyme inactivation rather than by the lixiviation of the NADH, which is still covalently bound to the support through boronic-diol complexation, even after being flushed with high ionic strength media for more than one day.

A self-sufficient heterogeneous three enzymes-two co-factors system for the amination of aldehydes. As a final step of our studies, we designed a more complex self-sufficient enzyme cascade where the ssHB(B)$_1$ containing AlaDH, FDH and NADH (14.4 μmol g^{-1}) supplies the amine donor (L-Alanine) to the His-tagged amine transaminase from *Pseudomonas fluorescens* (ATA) co-immobilized with PLP (9.8 μmol g^{-1}, system 3, **Table 1**) to concurrently aminate benzaldehyde to benzylamine as model reaction (**Figure 5a**). In this formal reductive amination, ammonium formate buffer acts as the primary source of hydride for FDH to *in situ* recycle NADH, and as an amine donor for AlaDH to reductively aminate pyruvate, thus synthesizing the L-Alanine demanded by ATA.[39] In this cascade, the reductive amination of pyruvate must occur first and in parallel with the NADH recycling, to concurrently enable the amination of benzaldehyde.

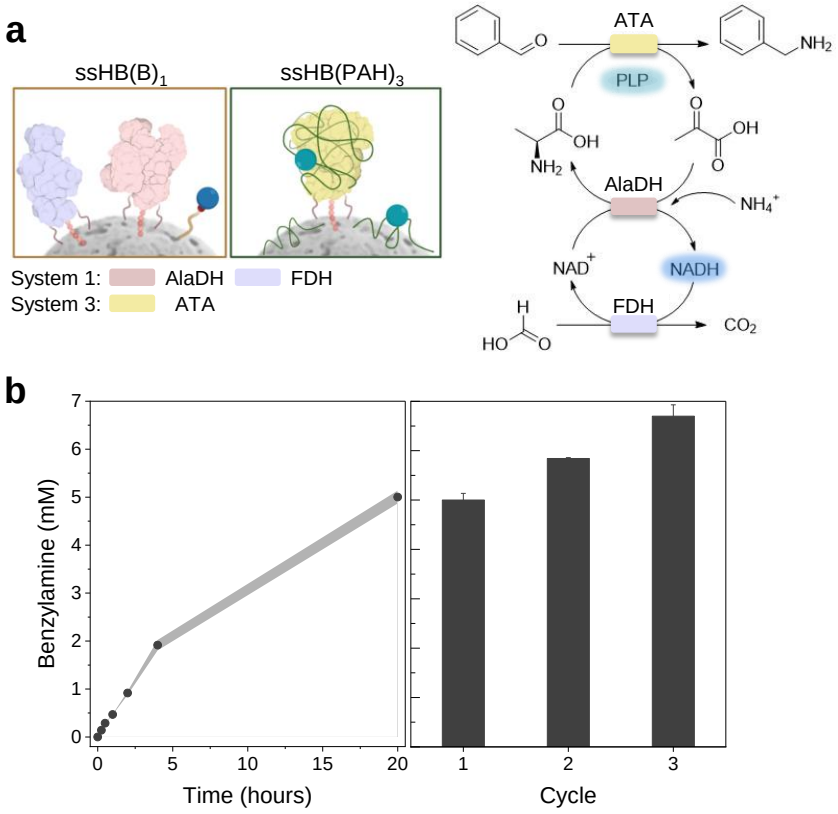

Figure 5. a) Schematic illustration of the ssHB(B)$_1$ and ssHB(PAH)$_2$ and the reaction scheme of the formal reductive amination of benzyaldehyde catalyzed by AlaDH, FDH, and ATA. **b)** Reaction course (left) of benzylamine synthesis catalyzed by the ssHB consortium shown in panel **(a)** and its recycling in consecutive batch cycles (right). Each cycle of 24 hours is performed with a fresh reaction mixture composed of 10 mM benzaldehyde, 0.5 M ammonium formate, and 75 mM pyruvate in 100 mM potassium phosphate buffer pH 8 at 25 ºC.

As PLP lacks a ribose group in its chemical structure to establish reversible bonds with the boronic acids of AG-B/Co^{2+}, the co-immobilization of the three enzymes and the two cofactors (NADH and PLP) in one single biocatalyst is not trivial. Thus, we decided to co-immobilize ATA and PLP on agarose beads functionalized with cobalt chelates and coated with polyallylamine (PAH). In this system, denoted as system 3, the His-tagged ATA is anchored to the support through metal-histidine coordination bonds, whereas the PLP is reversibly bound to the PAH polymeric layer through a dual mode; electrostatic interactions with the phosphate groups and imine covalent bonds with the aldehyde of PLP. As previously demonstrated by our group, the dual interaction mode that rules the binding of PLP with similar cationic polymers decreases the lixiviation of PLP even in the presence of high salt concentration (i.e., 1 M NaCl).[12] Furthermore, we previously reported that PLP co-immobilized on PAH exhibits a suitable association/dissociation equilibrium to become available for the immobilized ATA within the pore volume of the support.[13] In this study, we loaded 3.6 mg g^{-1} of ATA and 9.8 µmol g^{-1} of PLP (**Table 1**) on AG-PAH/Co^{2+}, which gives rise to the self-sufficient heterogeneous biocatalysts denoted as ssHB(PAH)$_3$. To note, ATA-driven amination often starts with an excess of the amine donor (i.e., L-Alanine) otherwise the reaction is thermodynamically unfavored.[40, 41] In contrast, we challenged the consortium of the two ssHBs with an excess of pyruvate instead of L-Alanine. Despite these unfavorable conditions, we found that the cascade is feasible in batch mode starting with 10 mM of benzaldehyde, 0.5 M ammonium formate, and 75 mM pyruvate in 0.1 M potassium phosphate buffer pH 8 at 25 ºC.

After 20 hours of reaction, the system reaches 5 mM benzylamine (50% chromatographic yield) (**Figure 5b)**. Remarkably, the two heterogeneous biocatalysts could be re-used for three consecutive batch cycles at their maximum performance without adding exogenous cofactors. These data demonstrate that both enzymes and cofactors can be successfully recycled. This is the first time where a combined system of ATAs and dehydrogenases work in the absence of exogenously supplied NAD(P)H and PLP cofactors in repeated batch biotransformations. Although the amine yield is lower than figures reported for similar systems using free cofactors and an excess of L-Alanine or other amine donors like isopropyl amine,[42, 43] we demonstrate that by confining enzymes and their corresponding cofactors, we can boost cascade reactions even under unfavorable thermodynamic conditions. Moreover, we open a new path to valorize biobased pyruvate, produced by engineered microbial strains as amine shuttle in amination reactions.[44]

CONCLUSIONS

Boronic acid-diol interaction enables the covalent and reversible co-immobilization of adenylated cofactors with their corresponding His-tagged enzymes on agarose porous microparticles functionalized with phenyl boronic acids and cobalt-chelates. The resulting heterogeneous biocatalysts are self-sufficient as they do not require the exogenous supply of cofactors. Upon spectroscopy and lixiviation studies, we demonstrate that adenylated cofactors react with supported boronic acids forming boronate esters, which withstand high ionic strength conditions. Using the herein prepared heterofunctional support, we fabricated self-sufficient heterogeneous biocatalysts that can perform different biotransformations under high ionic strength conditions without the exogenous addition of free cofactors. The boronic acid-diol complexation outperforms the widely exploited ionic interactions to enable, under high ionic conditions, the shuttle of the cofactors from the solid surface to the active site of the immobilized enzymes within the intraporal space without lixiviating them from the porous surface of their support. This new methodology opens a new operational window for amine and aminoacid dehydrogenases, but also for NAD(P)H recycling dehydrogenases that rely on substrates with increased salinity (i.e., ammonium formate or sodium phosphite). Furthermore, we prove the reusability of the bound cofactors both in batch and flow reaction modes under high salt concentration, reaching accumulated cofactor TTN in the range of hundreds. Although they are still far from the numbers reported for the self-sufficient heterogeneous biocatalyst where cofactors are electrostatically bound, these innovative biocatalysts allow reusing enzymes and cofactors for biotransformations where combined reuse is restricted (i.e., reductive amination with *in situ* NAD(P)H recycling).[14, 15] Using similar architectures as the herein reported, by implementing more active and stable enzymes, we anticipate the increment of cofactors´ TTN into the thousands.

MATERIALS AND METHODS

Functionalization of porous agarose microbeads with epoxy, cobalt-chelate, and boronic groups. For the immobilization of His-tagged enzymes on the agarose microbeads, the latter were activated with epoxy groups and iminodiacetic acid (IDA), as described elsewhere (**Figure S1a**).[12] The microbeads were incubated for different times and pH values, depending on the desired activation degree of epoxy and IDA groups (**Figure S1b**). Then, the epoxy and IDA-activated microbeads were incubated for 1 hour with $CoCl_2$ in an aqueous solution (30 mg mL^{-1}) resulting in a heterofunctional support containing both reactive Co^{2+}

chelates and epoxy groups (AG-E/Co^{2+}). Subsequently, the heterofunctional supports were incubated overnight (O/N) in 100 mM 3-APBA diluted in 20% isopropanol and 100 mM bicarbonate buffered solution at pH 11 (suspension ration 1:10 w:v). The boronic acid and Co^{2+} heterofunctional supports (AG-B/Co^{2+}) were washed with pure water and equilibrated in the cofactor immobilization buffer prior to cofactor binding. For the immobilization through electrostatic interactions, the supports were coated with a cationic polymer (PEI or PAH) upon the enzyme immobilization following our protocols described elsewhere.[13, 45] The supports were analyzed by X-ray photoelectron spectroscopy as described in supporting information. More details in support functionalization can be found in supporting information.

Solid-state NMR measurements. NMR spectra were derived using a Bruker Avance III WB400 spectrometer, employing 4 mm zirconia rotors that were rotated at a magic angle within a nitrogen environment at a frequency of 10 kHz. ^{11}B (128.39 MHz) and ^{31}P (161.99 MHz) spectra were measured by direct polarization with spinal64 ^{1}H high power decoupling sequence of 5 μs pulse length. The $\pi/2$ pulse lengths were 8.0 and 4.2 μs for ^{11}B and ^{31}P respectively.

Enzyme immobilization and co-immobilization. Enzymes were expressed, purified, labelled when needed, and functionalized characterized as described in supporting information. Unlabelled or RhB-labelled His-tagged enzymes (0.1 – 1 mg mL^{-1}) were incubated for 1 hour under orbital shaking with AG-B-/Co^{2+} or AG-E/Co^{2+} supports at a suspension of 1:10 w/v in 25 mM sodium phosphate buffer pH 7 and 25 ºC. After enzyme immobilization, the supports were washed 3 times with 10 volumes of the buffer used for immobilization. The immobilization yield (Ψ %) refers to the proportion of the provided enzyme that is immobilized on the carrier. It is computed using the following formula: Ψ = ((Offered enzyme concentration – Enzyme concentration in supernatant)/Offered enzyme concentration)*100. In the case of ATA, the immobilization protocol was the same, but the buffer of immobilization always included 0.1 mM of PLP to preserve its stability.[12, 46, 47] For the co-immobilization of AlaDH and FDH on the AG-B-/Co^{2+} supports we first incubated AlaDH (0.1 mg mL^{-1}) followed by the FDH (1 mg mL^{-1}). When they were co-immobilized on the AG-E/Co^{2+}, we first immobilized AlaDH and then the heterogeneous biocatalyst was coated with PEI (10 mg mL^{-1}) in HEPES 10 mM at pH 8 for 1 hour. Finally, the coated biocatalysts were washed with HEPES 10 mM pH 8, to remove any uncoated polymer and then incubated with FDH (1 mg mL^{-1}) for 1 hour in 25 mM phosphate buffer pH 7. Finally, all supports were washed with 25 mm sodium phosphate buffer pH 7 and stored at 4 ºC. Immobilized enzymes were analyzed previous their use and post-use by SDS-PAGE as described in supporting information.

Cofactor immobilization and lixiviation studies. Reversible immobilization of adenylated cofactors was explored by incubating 1-10 mM cofactor solution in different buffers incubated with AG-B/Co^{2+} in a 10:1 (v:w) suspension. Different incubation times and types of buffers are all shown in **Table S1**. For all cases, the mixture was subjected to orbital agitation at a rate of 25 rpm at room temperature. Subsequently, it was filtered and subjected to three rounds of washing using the appropriate buffer. The concentration of the immobilized cofactors was determined by measuring the absorbance of the supernatants following adsorption and after the three washing steps. This was done at wavelengths specific to each cofactor: 340 nm for NADH, 260 nm for NAD^+, 450 nm for FAD, 280 nm for ATP and $NADP^+$, and 390 nm for PLP. The measurements were recorded using an Epoch 2 Microplate Spectrophotometer from BioTek instruments. The load of the cofactor was calculated using the following equation:

$Cofactor\ load\ (\mu mol\ x\ g-1) = \left([cofactor]_{offered} - [cofactor]_{supernatant}\right) x \left(\frac{Bulk\ volume}{Carrier\ mass}\right)$, where solution is the concentration of the cofactor in the solutions of the flow through and the 3 washing steps. For each case, the lixiviation of the cofactors was monitored by conducting successive washing steps after the immobilization process, with absorbance measurements taken during each washing step. Similarly, we evaluated the immobilization yield and lixiviation of ionically adsorbed NADH or PLP on AG-E/Co^{2+} supports coated with PEI or PAH, respectively. The binding thermodynamics of cofactors were assessed as described in supporting information.

All self-sufficient heterogeneous biocatalyst developed in this study were analyzed at single-particle level by operando time-lapse fluorescence microscopy (see supporting information).

Synthesis of L-Alanine in batch mode. Batch mode synthesis of L-Alanine was done following protocols described elsewhere.[48] A quantity of 50 mg of the heterogeneous biocatalyst was loaded into a 1.5 mL Bio-spinTM column, along with 0.5 mL of a reaction mixture containing 0.5 M ammonium formate and 75 mM pyruvate in a potassium phosphate buffer (pH 8, 50 mM). The setup was then incubated at a temperature of 25 ºC using a vertical rotating shaker, operating at 30 rpm. When specified, exogenous 1.5 mM NADH supplementation was initially added to the reaction mixture. Each reaction course was monitored by taking samples at different time intervals which were filtered through a 10 kDa tangential filtration unit and properly diluted prior to their derivatization for HPLC analysis.

The reaction courses shown in **Figure 4b** show the change in concentration of L-Alanine, [P], versus time, which follows an exponential growth, yielding to an observed rate constant, k_{obs}, that depends on the initial concentration of the substrate, A_o. To obtain the $k_{obs,}$ we fitted the data from L-Ala biosynthesis time courses to a first-order reaction (Equation 1). Fitting with Equation 1 was done using OriginLab.[49]

$$[P] = A_o - A_o e^{-k_{obs}t} \qquad \text{Equation 1}$$

Synthesis of L-Analine in a PBR in flow mode. The heterogeneous biocatalyst (900 mg, corresponding to 1.26 mL) was loaded into a column measuring 2 x 0.4 cm and subsequently linked to a flow system. A reaction mixture composed of 50/500 mM ammonium formate and 7.5/75 mM pyruvate in 50 mM potassium phosphate buffer pH 8 was passed through the column at 25µL min^{-1}. Samples were collected from the outlet at different time points and then properly diluted, derivatized, and analyzed by chiral HPLC. The space-time yield (STY) was calculated by dividing the L-Ala concentration in the outlet between the residence time of the reactor (τ), which is defined as the reactor volume divided by the flow rate.

Synthesis of benzylamine and 4-aminobutyric in batch mode. For the synthesis of benzylamine, the biocatalysts $ssHB(B)_1$ and $ssHB(PAH)_2$ (100 mg each) were placed inside a Bio-spinTM column of 1.5 mL volume with 0.8 mL of a reaction mixture containing 10 mM benzaldehyde (stock 1 M in DMSO), 0.5 M ammonium formate and 75 mM pyruvate in 100 mM potassium phosphate buffer pH 8. Accordingly, for the synthesis of 4-aminoburic acid, the $ssHB(B)_2$ (100 mg) was placed in the corresponding column with 1.0 mL of reaction mixture containing 100 mM lithium acetoacetate (stock 1 M in water), 0.5 M ammonium chloride and 1 M isopropanol in 100 mM sodium bicarbonate buffer pH 9. and incubated at 25 ºC in a vertical rotating shaker at 30 rpm. The columns were rotated vertically at 30 rpm. The reaction

courses were monitored by taking samples at different time points which were filtered through a 10 kDa tangential filtration unit and properly diluted prior to HPLC analysis. For the synthesis of 4-aminoburic acid controls were performed with the free enzymes and cofactor, at the same concentrations of immobilized protein (1 mg and 0.5 mg of AmDH and KRED, respectively) and NADPH (1.6 mM) on the ssHB$(B)_2$.

HPLC measurements for L-Alanine quantification. The concentration of L-alanine and S-4-aminobutyric acid was quantified by chiral derivatization with Marfey reagent and analyzed by HPLC. Briefly, 20 µL of aqueous sample (0.6 - 10 mM) were mixed with 8 µL of 1 M sodium bicarbonate and 20 µL of 15 mM Marfey's reagent (Cat. 48895, Thermofisher) in acetone and incubated for 50 min at 50 ºC. Afterward, 8 µL of 1 M HCl was added and then centrifuged for 10 min at 13450 g. Finally, samples were diluted with 75 µL acetonitrile and properly filtered. HPLC analysis was conducted as described elsewhere.[50] The samples were monitored at a wavelength of 340 nm and eluted with a flow rate of 1 mL min^{-1} using a dual mobile-phase system. Mobile phase A consisted of 0.1% trifluoroacetic acid in water, while mobile phase B comprised acetonitrile. Elution conditions for samples containing L-Alanine: Starting with 90% A and 10% B, followed by increasing constant rate from 90% to 80% A in 17 min, maintained for 3 min, then remained in constant increasing rate from 80% to 60% of A for 20 more minutes and then restored the initial conditions for 20 more minutes. The retention time of L-Alanine: 25.6 min. Elution conditions for samples containing 4-aminobutyric acid: Isocratic 70% A and 30% of B during 15 min. Retention times: *S*-4 aminobutyric acid: 4,65 min, and *R*-4 aminobutyric acid: 6,62 min.

HPLC measurements for benzaldehyde and pyruvate quantification. Benzaldehyde and pyruvate synthesis in batch mode, were quantified by HPLC.[50] Samples containing benzaldehyde were diluted by a 10 to 100 factor in a mix of water/acetonitrile 30/70 (v:v), while pyruvate samples were diluted in 50 mM sodium phosphate buffer at pH 2.9. The samples were monitored at 254 nm (Benzaldehyde) and 220 nm (pyruvate)) and were eluted at 1- and 0.7-mL min^{-1} flow rates respectively, using two mobile phases for benzaldehyde detection as described for L-Alanine. For pyruvate detection one mobile phase was used (A) composed by 50 mM sodium phosphate buffer at pH 2.9. Elution conditions for benzaldehyde, Isocratic at 70% A and 30% B for 15 min; elution conditions for pyruvate: Isocratic at 100% A for 15 min. Retention times: pyruvate: 1.64 min, benzaldehyde 3.75 min

ASSOCIATED CONTENT

Supporting Information. Additional materials and Methods and experimental results are shown as supporting Figures and Tables as well as XPS, NMR spectra, and chromatograms of the compounds herein used. This material is available free of charge via the Internet at http://pubs.acs.org

AUTHOR INFORMATION

Corresponding Author

*__Fernando López Gallego__ – Center for cooperative Research in Biomaterials (CIC biomaGUNE) - Basque Research and Technology Alliance (BRTA) Paseo Miramón, 194, 20014 Donostia-San Sebastián, Spain.

Email: flopez@cicbiomagune.es

Author Contributions

‡**Eleftheria Diamanti** – Center for Cooperative Research in Biomaterials (CIC biomaGUNE) - Basque Research and Technology Alliance (BRTA) Paseo Miramón, 194, 20014 Donostia-San Sebastián, Spain.
‡**Susana Velasco-Lozano** – Departamento de Química Orgánica, Instituto de Síntesis Química y Catálisis Homogénea (ISQCH), Universidad de Zaragoza-CSIC, Pedro Cerbuna 12, E-50009, Zaragoza, Spain - Aragonese Foundation for Research and Development (ARAID), Zaragoza, Spain.
Daniel Grajales-Hernández – Center for cooperative Research in Biomaterials (CIC biomaGUNE) - Basque Research and Technology Alliance (BRTA) Paseo Miramón, 194, 20014 Donostia-San Sebastián, Spain.
Alejandro Herrera Orrego – Center for cooperative Research in Biomaterials (CIC biomaGUNE) - Basque Research and Technology Alliance (BRTA) Paseo Miramón, 194, 20014 Donostia-San Sebastián, Spain.
Desiré Di Silvio – Center for cooperative Research in Biomaterials (CIC biomaGUNE) - Basque Research and Technology Alliance (BRTA) Paseo Miramón, 194, 20014 Donostia-San Sebastián, Spain.
José María Fraile – Instituto de Síntesis Química y Catálisis Homogénea (ISQCH), Universidad de Zaragoza-CSIC, Pedro Cerbuna 12, E-50009, Zaragoza, Spain.

‡ These authors contributed equally.

Notes
The authors declare no competing financial interest.

ACKNOWLEDGMENTS

This work has received funding from the European Research Council (ERC) under the European Union's Horizon 2020 research and innovation program (Grant Agreement No. 818089). F.L.-G. acknowledges the funding of IKERBASQUE and the Spanish State Research Agency (AIE) (RTI2018- 094398-B-I00). A.H.O. thanks BIKAINTEK program (Basque Government) for co-funding him. S.V.-L. acknowledges the funding received from ARAID Foundation. D.G.H acknowledges the funding received from CONACYT postdoctoral program. This work was supported by the Spanish Ministry of Science and Innovation under the Maria de Maeztu Units of Excellence Program (MDM-2017-0720).

REFERENCES

(1) Alcantara, A. R.; Dominguez de Maria, P.; Littlechild, J. A.; Schurmann, M.; Sheldon, R. A.; Wohlgemuth, R. Biocatalysis as Key to Sustainable Industrial Chemistry. *ChemSusChem* **2022**, *15* (9), 202102709.
(2) Heidlindemann, M.; Rulli, G.; Berkessel, A.; Hummel, W.; Gröger, H. Combination of Asymmetric Organo- and Biocatalytic Reactions in Organic Media Using Immobilized Catalysts in Different Compartments. *ACS Catal.* **2014**, *4* (4), 1099-1103.
(3) Zhang, Y.-Q.; Feng, T.-T.; Cao, Y.-F.; Zhang, X.-Y.; Wang, T.; Huanca Nina, M. R.; Wang, L.-C.; Yu, H.-L.; Xu, J.-H.; Ge, J.; et al. Confining Enzyme Clusters in Bacteriophage P22 Enhances Cofactor Recycling and Stereoselectivity for Chiral Alcohol Synthesis. *ACS Catal.* **2021**, *11* (16), 10487-10493.
(4) Zhou, N.; Wei, G.; Chen, X.; Wu, B.; Li, H.; Lu, Q.; Cao, X.; Zhang, A.; Chen, K.; Ouyang, P. Self-sufficient biocatalysts constructed using chitin-based microspheres. *Chem. Eng. J.* **2023**, *459*, 141660.
(5) Wei, W.; Ettelaie, R.; Zhang, X.; Fan, M.; Dong, Y.; Li, Z.; Yang, H. Co-compartmentalization of Enzymes and Cofactors within Pickering Emulsion Droplets for Continuous-Flow Catalysis. *Angew. Chem. Int. Ed. Engl.* **2022**, *61* (45), e202211912. (accessed 2022/10/12)

(6) Benítez-Mateos, A. I.; San Sebastian, E.; Ríos-Lombardía, N.; Morís, F.; González-Sabín, J.; López-Gallego, F. Asymmetric Reduction of Prochiral Ketones by Using Self-Sufficient Heterogeneous Biocatalysts Based on NADPH-Dependent Ketoreductases. *Chem. Eur. J.* **2017**, *23* (66), 16843-16852.
(7) Schmid-Dannert, C.; López-Gallego, F. Advances and opportunities for the design of self-sufficient and spatially organized cell-free biocatalytic systems. *Curr. Opin. Chem. Biol.* **2019**, *49*, 97-104.
(8) Velasco-Lozano, S.; Benítez-Mateos, A. I.; López-Gallego, F. Co-immobilized Phosphorylated Cofactors and Enzymes as Self-Sufficient Heterogeneous Biocatalysts for Chemical Processes. *Angew. Chem. Int. Ed.* **2017**, *56* (3), 771-775.
(9) Cha, J.; Cho, J.; Kwon, I. Self-Sufficient Reusable Biocatalytic System Outfitted with Multiple Oxidoreductases and Flexible Polypeptide-Based Cofactor Swing Arms. *ACS Sustain. Chem. Eng.* **2023**, *11* (9), 3710-3719.
(10) Hartley, C. J.; Williams, C. C.; Scoble, J. A.; Churches, Q. I.; North, A.; French, N. G.; Nebl, T.; Coia, G.; Warden, A. C.; Simpson, G.; et al. Engineered enzymes that retain and regenerate their cofactors enable continuous-flow biocatalysis. *Nat. Catal.* **2019**, *2* (11), 1006-1015.
(11) Benítez-Mateos, A. I.; Huber, C.; Nidetzky, B.; Bolivar, J. M.; López-Gallego, F. Design of the Enzyme–Carrier Interface to Overcome the O 2 and NADH Mass Transfer Limitations of an Immobilized Flavin Oxidase. *ACS Appl. Mater. Interfaces* **2020**, *12* (50), 56027-56038.
(12) Benítez-Mateos, A. I.; Contente, M. L.; Velasco-Lozano, S.; Paradisi, F.; López-Gallego, F. Self-Sufficient Flow-Biocatalysis by Coimmobilization of Pyridoxal 5′-Phosphate and ω-Transaminases onto Porous Carriers. *ACS Sustain. Chem. Eng.* **2018**, *6* (10), 13151-13159.
(13) Diamanti, E.; Santiago-Arcos, J.; Grajales-Hernández, D.; Czarnievicz, N.; Comino, N.; Llarena, I.; Di Silvio, D.; Cortajarena, A. L.; López-Gallego, F. Intraparticle Kinetics Unveil Crowding and Enzyme Distribution Effects on the Performance of Cofactor-Dependent Heterogeneous Biocatalysts. *ACS Catal.* **2021**, *11* (24), 15051-15067.
(14) Roura Padrosa, D.; Benítez-Mateos, A. I.; Calvey, L.; Paradisi, F. Cell-free biocatalytic syntheses of l-pipecolic acid: a dual strategy approach and process intensification in flow. *Green Chem.* **2020**, *22* (16), 5310-5316.
(15) Velasco-Lozano, S.; da Silva, E. S.; Llop, J.; López-Gallego, F.; Lopez-Gallego, F. Sustainable and Continuous Synthesis of Enantiopure l-Amino Acids by Using a Versatile Immobilised Multienzyme System. *ChemBioChem* **2018**, *19* (4), 395-403.
(16) Liu, S.; Wang, Z.; Chen, K.; Yu, L.; Shi, Q.; Dong, X.; Sun, Y. Cascade chiral amine synthesis catalyzed by site-specifically co-immobilized alcohol and amine dehydrogenases. *Catal. Sci. Tech.* **2022**, *12* (14), 4486-4497.
(17) Franklin, R. D.; Whitley, J. A.; Caparco, A. A.; Bommarius, B. R.; Champion, J. A.; Bommarius, A. S. Continuous production of a chiral amine in a packed bed reactor with co-immobilized amine dehydrogenase and formate dehydrogenase. *Chem. Eng. J.* **2021**, *407*, 127065.
(18) Andexer, J. N.; Richter, M. Emerging enzymes for ATP regeneration in biocatalytic processes. *ChemBioChem* **2015**, *16* (3), 380-386.
(19) Croci, F.; Vilim, J.; Adamopoulou, T.; Tseliou, V.; Schoenmakers, P. J.; Knaus, T.; Mutti, F. G. Continuous Flow Biocatalytic Reductive Amination by Co-Entrapping Dehydrogenases with Agarose Gel in a 3D-Printed Mould Reactor. *ChemBioChem* **2022**, *23* (22), e202200549.
(20) Mattey, A. P.; Ford, G. J.; Citoler, J.; Baldwin, C.; Marshall, J. R.; Palmer, R. B.; Thompson, M.; Turner, N. J.; Cosgrove, S. C.; Flitsch, S. L. Development of Continuous Flow Systems to Access Secondary Amines Through Previously Incompatible Biocatalytic Cascades**. *Angew. Chem. Int. Ed.* **2021**, *60* (34), 18660-18665.
(21) Vrtis, J. M.; White, A. K.; Metcalf, W. W.; van der Donk, W. A. Phosphite Dehydrogenase: A Versatile Cofactor-Regeneration Enzyme. *Angew. Chem. Int. Ed.* **2002**, *41* (17), 3257-3259.
(22) Springsteen, G.; Wang, B. A detailed examination of boronic acid–diol complexation. *Tetrahedron* **2002**, *58* (26), 5291-5300.
(23) Brooks, W. L. A.; Deng, C. C.; Sumerlin, B. S. Structure–Reactivity Relationships in Boronic Acid–Diol Complexation. *ACS Omega* **2018**, *3* (12), 17863-17870.
(24) Kim, D. H.; Marbois, B. N.; Faull, K. F.; Eckhert, C. D. Esterification of borate with NAD+ and NADH as studied by electrospray ionization mass spectrometry and11B NMR spectroscopy. *J. Mass Spectrom.* **2003**, *38* (6), 632-640.
(25) Kim, D. H.; Faull, K. F.; Norris, A. J.; Eckhert, C. D. Borate-nucleotide complex formation depends on charge and phosphorylation state. *J. Mass Spectrom.* **2004**, *39* (7), 743-751.
(26) Kim, D. H.; Eckhert, C. D.; Faull, K. F. Utilization of Negative Ion ESI-MS and Tandem Mass Spectrometry To Detect and Confirm the NADH−Boric Acid Complex. *J. Chem. Educ.* **2010**, *88* (1), 106-110.

(27) Akgun, B.; Hall, D. G. Boronic Acids as Bioorthogonal Probes in Site- Selective Labeling of Proteins. *Angew. Chem.* **2018**, *130* (40), 13210-13228.
(28) Hernández-Paredes, J.; Olvera-Tapia, A. L.; Arenas-García, J. I.; Höpfl, H.; Morales-Rojas, H.; Herrera-Ruiz, D.; Gonzaga-Morales, A. I.; Rodríguez-Fragoso, L. On molecular complexes derived from amino acids and nicotinamides in combination with boronic acids. *Cryst. Eng. Comm.* **2015**, *17* (28), 5166-5186.
(29) Chen, W.-H.; Vázquez-González, M.; Zoabi, A.; Abu-Reziq, R.; Willner, I. Biocatalytic cascades driven by enzymes encapsulated in metal–organic framework nanoparticles. *Nat. Catal.* **2018**, *1* (9), 689-695.
(30) Zayats, M.; Katz, E.; Willner, I. Electrical contacting of glucose oxidase by surface-reconstitution of the apo-protein on a relay-boronic acid-FAD cofactor monolayer. *J. Am. Chem. Soc.* **2002**, *124* (10), 2120-2121.
(31) Martins de Oliveira, S.; Velasco-Lozano, S.; Orrego, A. H.; Rocha-Martin, J.; Moreno-Perez, S.; Fraile, J. M.; Lopez-Gallego, F.; Guisán, J. M. Functionalization of porous cellulose with glyoxyl groups as a carrier for enzyme immobilization and stabilization. *Biomacromolecules* **2021**, *22* (2), 927-937.
(32) Weiss, J. W.; Bryce, D. L. A solid-state (11)b NMR and computational study of boron electric field gradient and chemical shift tensors in boronic acids and boronic esters. *J. Phys. Chem. A* **2010**, *114* (15), 5119-5131.
(33) Rover, L.; Fernandes, J. C. B.; Neto, G. D. O.; Kubota, L. T.; Katekawa, E.; Serrano, S. H. P. Study of NADH stability using ultraviolet-visible spectrophotometric analysis and factorial design. *Anal. Biochem.* **1998**, *260* (1), 50-55.
(34) Galkin, A.; Kulakova, L.; Yoshimura, T.; Soda, K.; Esaki, N. Synthesis of optically active amino acids from alpha-keto acids with Escherichia coli cells expressing heterologous genes. *Appl. Environ. Microbiol.* **1997**, *63* (12), 4651-4656.
(35) Hanson, R. L.; Goldberg, S. L.; Brzozowski, D. B.; Tully, T. P.; Cazzulino, D.; Parker, W. L.; Lyngberg, O. K.; Vu, T. C.; Wong, M. K.; Patel, R. N. Preparation of an Amino Acid Intermediate for the Dipeptidyl Peptidase IV Inhibitor, Saxagliptin, using a Modified Phenylalanine Dehydrogenase. *Adv. Synth. Catal.* **2007**, *349* (8-9), 1369-1378.
(36) Hanson, R. L.; Howell, J. M.; LaPorte, T. L.; Donovan, M. J.; Cazzulino, D. L.; Zannella, V.; Montana, M. A.; Nanduri, V. B.; Schwarz, S. R.; Eiring, R. F.; et al. Synthesis of allysine ethylene acetal using phenylalanine dehydrogenase from Thermoactinomyces intermedius. *Enzyme Microb. Technol.* **2000**, *26* (5-6), 348-358.
(37) Turnover number, TTN = [L-Alanine] / [NADH] or [AlaDH]. In all cases TTN for AlaDH is determined with the immobilized enzymes, while for the NADH we determined this parameter for both the free and immobilized NADH.
(38) Peschke, T.; Bitterwolf, P.; Gallus, S.; Hu, Y.; Oelschlaeger, C.; Willenbacher, N.; Rabe, K. S.; Niemeyer, C. M. Self-Assembling All-Enzyme Hydrogels for Flow Biocatalysis. *Angew. Chem. Int. Ed. Engl.* **2018**, *57* (52), 17028-17032.
(39) Koszelewski, D.; Lavandera, I.; Clay, D.; Guebitz, G. M.; Rozzell, D.; Kroutil, W. Formal asymmetric biocatalytic reductive amination. *Angew. Chem. Int. Ed. Engl.* **2008**, *47* (48), 9337-9340.
(40) Kelly, S. A.; Pohle, S.; Wharry, S.; Mix, S.; Allen, C. C. R.; Moody, T. S.; Gilmore, B. F. Application of ω-Transaminases in the Pharmaceutical Industry. *Chem. Rev.* **2018**, *118* (1), 349-367.
(41) Slabu, I.; Galman, J. L.; Lloyd, R. C.; Turner, N. J. Discovery, Engineering, and Synthetic Application of Transaminase Biocatalysts. *ACS Catal.* **2017**, *7* (12), 8263-8284.
(42) Richter, N.; Farnberger, J. E.; Pressnitz, D.; Lechner, H.; Zepeck, F.; Kroutil, W. A system for ω-transaminase mediated (R)-amination usingl-alanine as an amine donor. *Green Chem.* **2015**, *17* (5), 2952-2958.
(43) Kohls, H.; Anderson, M.; Dickerhoff, J.; Weisz, K.; Córdova, A.; Berglund, P.; Brundiek, H.; Bornscheuer, U. T.; Höhne, M. Selective Access to All Four Diastereomers of a 1,3-Amino Alcohol by Combination of a Keto Reductase- and an Amine Transaminase-Catalysed Reaction. *Adv. Synth. Catal.* **2015**, *357* (8), 1808-1814.
(44) Labib, M.; Grabowski, L.; Brüsseler, C.; Kallscheuer, N.; Wachtendonk, L.; Fuchs, T.; Jupke, A.; Wiechert, W.; Marienhagen, J.; Rother, D.; et al. Toward the Sustainable Production of the Active Pharmaceutical Ingredient Metaraminol. *ACS Sustain. Chem. Eng.* **2022**, *10* (16), 5117-5128.
(45) Muñoz-Morales, E.; Velasco-Lozano, S.; Benítez-Mateos, A. I.; Marín, M. J.; Ramos-Cabrer, P.; López-Gallego, F. Deciphering the Effect of Microbead Size Distribution on the Kinetics of Heterogeneous Biocatalysts through Single-Particle Analysis Based on Fluorescence Microscopy. *Catalysts* **2019**, *9* (11), 896.

(46) Velasco-Lozano, S.; Jackson, E.; Ripoll, M.; Lopez-Gallego, F.; Betancor, L. Stabilization of omega-transaminase from Pseudomonas fluorescens by immobilization techniques. *Int. J. Biol. Macromol.* **2020**, *164*, 4318-4328.
(47) Shin, J. S.; Yun, H.; Jang, J. W.; Park, I.; Kim, B. G. Purification, characterization, and molecular cloning of a novel amine:pyruvate transaminase from Vibrio fluvialis JS17. *Appl. Microbiol. Biotechnol.* **2003**, *61* (5-6), 463-471.
(48) Santiago-Arcos, J.; Velasco-Lozano, S.; Diamanti, E.; Cortajarena, A. L.; López-Gallego, F. Immobilization Screening and Characterization of an Alcohol Dehydrogenase and its Application to the Multi-Enzymatic Selective Oxidation of 1,-Omega-Diols. *Front. Catal.* **2021**, *1*, 9.
(49) *Origin*; OriginLab Corporation: Northampton MA, USA., 2020. (accessed.
(50) Santiago-Arcos, J.; Velasco-Lozano, S.; López-Gallego, F. Multienzyme Coimmobilization on Triheterofunctional Supports. *Biomacromolecules* **2023**, *24* (2), 929-942.

For Table of Contents Use Only

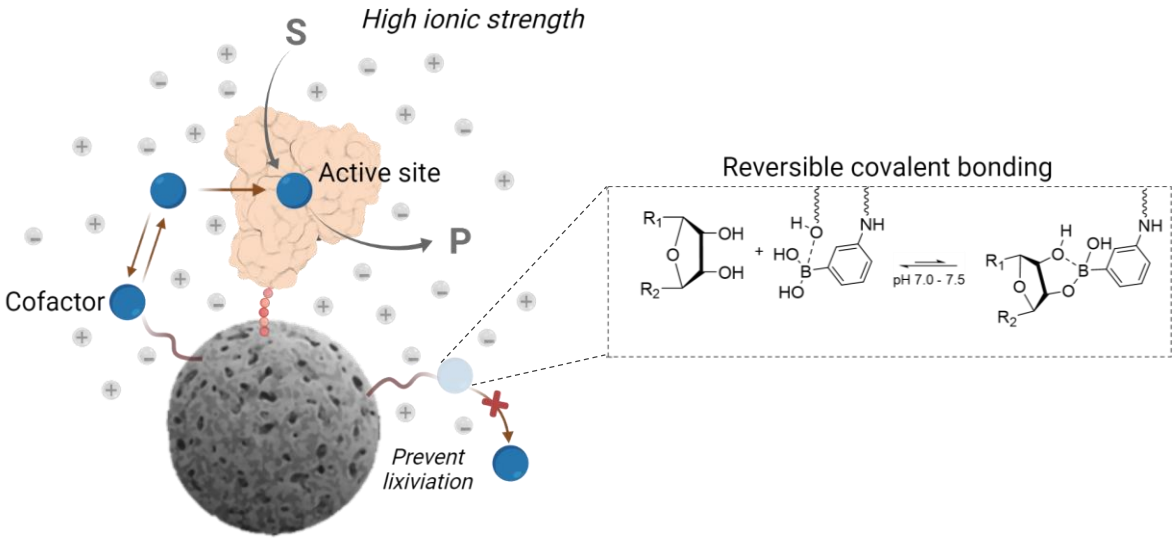

Boronic acid-diol complexation enables self-sufficient heterogeneous biocatalysts for biotransformations under high ionic strength, allowing both enzyme and cofactor reusability.